Chemiluminescence of the Ce(IV)/CDP-Star System Based on the Phosphatase-like Activity of Ce(IV) Ions

Lianzhe Hu,* Xilu Hu, Ting Huang, Min Wang,* and Guobao Xu*

ACCESS | Metrics & More | Article Recommendations | SI Supporting Information

ABSTRACT: The phosphatase-like activity of Ce(IV) ions was applied for chemiluminescence (CL) analysis for the first time. Ce(IV) can catalyze the hydrolysis of CDP-star, which is a phosphatase substrate, to produce strong CL emission. The CL performance of the Ce(IV)/CDP-star system can be significantly improved by the addition of ionic liquids. In the presence of 1-butyl-3-methylimidazolium tetrafluoroborate, the selective and sensitive CL detection of Ce(IV) ions was achieved with a detection limit of 460 nM. The proposed CL system was also used for the detection of ascorbic acid and ClO⁻. It is based on the phenomenon that Ce(IV) can catalyze the hydrolysis of CDP-star, while Ce(III) cannot. The introduction of reductive ascorbic acid into the mixture of Ce(IV)/CDP-star can turn off the CL signal, while the addition of oxidative ClO⁻ into the solution of Ce(III)/CDP-star can turn on the CL emission. Finally, Ce(IV)/CDP-star CL was successfully applied for evaluating the total antioxidant capacity in commercial fruit juice samples.
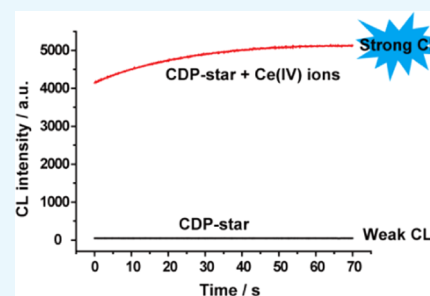
INTRODUCTION

Chemiluminescence (CL) is a light-emission phenomenon initiated by chemical reactions.[1] As a powerful analytical technology, CL has been widely used in a variety of areas including enzyme-linked immunoassays, forensic analysis, DNA probe detection, and bioimaging.[2−5] Most of the known CL systems produce light through redox reactions, such as the frequently investigated luminol CL, peroxyoxalate CL, and lucigenin CL systems.[6−8] These CL systems are usually activated by strong oxidizing reagents such as H_2O_2, potassium permanganate, and hypochlorites.[9−11] Nevertheless, these oxidizing reagents are easy to decompose due to their thermodynamic instability, which may result in poor reproducibility of the CL systems. Unlike other CL luminophores, the CL emission of phenoxy 1,2-dioxetane compounds is not oxidation dependent.[12] The light emission of phenoxy 1,2-dioxetane luminophores is triggered by the removal of the phenol-protecting group.[13−16] The most recognized phenoxy 1,2-dioxetane luminophore is CDP-star, which has been used as the substrate of alkaline phosphatase (ALP) in enzyme-linked immunoassays. In the presence of ALP, the CL of CDP-star is activated through enzyme-catalyzed phenol deprotection.[17] However, natural alkaline phosphatase has inherent drawbacks such as high cost in purification and low stability due to denaturation, which limit the broad applications of CDP-star CL.

Artificial enzyme mimics have received increasing attention due to their unique characteristics such as high stability and suitability for large-scale preparation. In recent years, nanomaterials with enzyme-like activity (nanozymes) have gained tremendous interest in the field of artificial enzymes.[18−20] Nanozymes have found wide applications in the fields of

cancer therapy, biosensors, bioimaging, and environmental protection.[21−28] Due to the excellent catalytic activity, nanoceria has attracted considerable attention among the currently available nanozymes.[29] Nanoceria has been reported to exhibit multienzyme-like activities, including superoxide oxidase, catalase, oxidase, laccase, and phosphatase mimetic activities.[30−32] The enzyme-like activities of nanoceria are usually demonstrated using chromogenic and/or fluorogenic substrates of natural enzymes.[33] Recently, the phosphatase-like activity of nanoceria was demonstrated using CDP-star as the CL substrate.[34] The nanoceria/CDP-star CL system has further been used for imaging of Al^{3+} in living cells. Nevertheless, nanoceria/CDP-star CL still has significant deficiencies. First, the nanoceria particles have poor solubility in aqueous solution and tend to aggregate during use. Second, different batches of nanoceria particles may show dissimilar catalytic activities, which would result in poor reproducibility in CL assays.

Herein, the Ce(IV)/CDP-star CL system is proposed based on the phosphatase-like activity of Ce(IV) ions instead of nanoceria particles. In the presence of Ce(IV) ions, dephosphorylation of CDP-star occurred and was accompanied with strong CL emission. In contrast, Ce(III) ions showed negligible phosphatase-like activity. The effect of ionic liquids
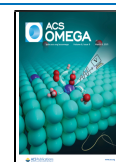
(ILs) on Ce(IV)/CDP-star CL was also investigated using 1-butyl-3-methylimidazolium tetrafluoroborate ([BMIM][BF$_4$]) as the model case. After introducing [BMIM][BF$_4$] into the system, the CL intensity of Ce(IV)/CDP-star was significantly increased. With the aid of [BMIM][BF$_4$], the sensitive and selective CL detection of Ce(IV) ions was demonstrated. Finally, the CL system was used for ascorbic acid (AA) and ClO$^-$ detection by utilizing the reversible Ce(III)/Ce(IV) redox switch. AA is an antioxidant, which has excellent reactive oxygen species (ROS) scavenging ability in living organisms.[35] The CL of Ce(IV)/CDP-star can be efficiently quenched by the addition of AA due to the reduction of Ce(IV) to Ce(III). ClO$^-$ is one kind of ROS that plays important roles in metabolic processes.[36] The addition of ClO$^-$ into the solution of Ce(III)/CDP-star will lead to the oxidation of Ce(III) to Ce(IV), which was accompanied with strong CL emission. To further demonstrate the practical usage of Ce(IV)/CDP-star CL, the CL detection of the total antioxidant capacity (TAC) in fruit juices was also achieved with satisfactory results.

■ RESULTS AND DISCUSSION

Phosphatase-like Activity of Ce(IV) Ions. CDP-star is a commercially available CL substrate of ALP. It can produce strong CL emission upon enzyme-catalyzed phenol deprotection. The phosphatase-like activity of nanoceria has been demonstrated using CDP-star as the CL substrate.[34] It is interesting to investigate the catalytic activity of Ce(III) and Ce(IV) ions because nanoceria particles have both Ce(III) and Ce(IV) on their surfaces. As shown in Figure 1, CDP-star itself
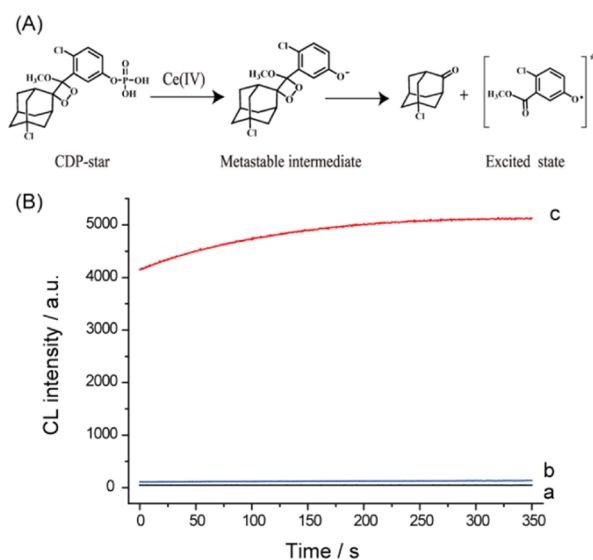
Figure 1. (A) Reaction scheme of Ce(IV) ion-catalyzed dephosphorylation of CDP-star. (B) CL kinetic curves of 25 μM CDP-star (a), 25 μM CDP-star in the presence of 600 μM Ce(III) ions (b), and 25 μM CDP-star in the presence of 600 μM Ce(IV) ions (c). The experiments were carried out in 20 mM N-(2-hydroxyethyl)-piperazine-N'-ethanesulfonic acid (HEPES) buffer (pH 7.0).

showed almost no CL emission in aqueous solution. However, strong CL emission was observed upon the addition of 600 μM Ce(IV) ions. In comparison, only a negligible CL signal appeared after the addition of 600 μM Ce(III) ions. This suggests that Ce(IV) ions have intrinsic phosphatase-like activity similar to nanoceria particles (Figure 1A), while the phosphatase-like activity of Ce(III) ions could almost be

ignored. The result is similar to a recent report using p-NPP as the chromogenic substrate.[32]

The catalytic activity of Ce(IV) ions was then studied under different pH values. Figure S1 shows the effect of pH on the CL intensity of 25 μM CDP-star in the presence of 600 μM Ce(IV) ions. The CL intensity of the Ce(IV)/CDP-star system increased with increasing pH until pH 7, and then the CL intensity decreased in alkaline pH conditions. This is different from the nanoceria/CDP-star CL system, which has an optimum condition of pH 9.0.[34] Ce(IV) ions tend to precipitate in alkaline solution, which may result in the decrease of Ce(IV)/CDP-star CL in alkaline solution. The robust CL emission of Ce(IV)/CDP-star at neutral pH is beneficial for its further application in biological samples. The phosphatase-like activity of Ce(IV) ions was then investigated using steady-state kinetics. As shown in Figure S2, a typical Michaelis–Menten curve was obtained for Ce(IV) ions with CDP-star as the CL substrate. The comparison of the kinetic parameters of Ce(IV) ions with nanoceria and ALP at pH 7 is shown in Table S1. The apparent K_m value of Ce(IV) ions with CDP-star as the substrate is even lower than that of nanoceria and ALP, although the K_{cat} of Ce(IV) ions is much lower. The CL intensities of 25 μM CDP-star in the presence of different concentrations of Ce(IV) ions at pH 7 are shown in Figure S3. The CL intensity of CDP-star increased with increasing concentrations of Ce(IV) ions in the range from 50 to 600 μM, and a detection limit of 39.51 μM for Ce(IV) ion detection was calculated (Figure S4).

Enhancement of Ce(IV)/CDP-Star CL by ILs. Recently, ILs have been used as a modulator in artificial enzymes or as a stabilizing mediator to thermally stabilize the enzymatic product.[37−39] The CL of the Ce(IV)/CDP-star system was then evaluated in the presence of ILs. A representative IL, [BMIM][BF$_4$], was selected as a model molecule. Figure 2
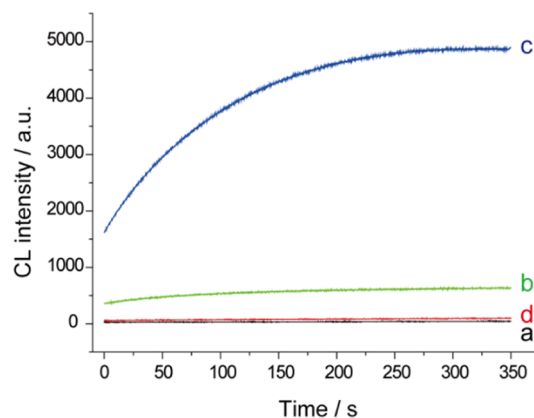
Figure 2. CL kinetic curves of 25 μM CDP-star (a), 25 μM CDP-star in the presence of 100 μM Ce(IV) ions (b), 25 μM CDP-star in the presence of 100 μM Ce(IV) ions and 2% (v/v) [BMIM][BF$_4$] (c), and 25 μM CDP-star in the presence of 2% (v/v) [BMIM][BF$_4$] (d).

shows the CL kinetic curves of 25 μM CDP-star and 100 μM Ce(IV) ions without and with the addition of [BMIM][BF$_4$]. In the presence of 2% (v/v) [BMIM][BF$_4$], the CL intensity of the Ce(IV)/CDP-star system was significantly increased. The effect of different amounts of [BMIM][BF$_4$] on the CL performance of the Ce(IV)/CDP-star system is shown in Figure S5. The CL of Ce(IV)/CDP-star increased with increasing concentrations of [BMIM][BF$_4$] in the range from

0.3 to 2% (v/v) and then decreased when the concentration of [BMIM][BF$_4$] was higher than 2% (v/v). Therefore, 2% (v/v) [BMIM][BF$_4$] was used in the following CL assays. The effect of [BMIM][BF$_4$] on the catalytic activity of Ce(IV) ions toward the dephosphorylation of fluorogenic and chromogenic substrates was also investigated. As shown in Figure S6, the fluorescence signals of the Ce(IV)/4-methylumbelliferyl phosphate system were decreased in the presence of [BMIM][BF$_4$], while the absorbance values of the Ce(IV)/p-nitrophenyl phosphate system were almost unchanged after the addition of [BMIM][BF$_4$]. This indicates that the addition of [BMIM][BF$_4$] could not improve the catalytic activity of Ce(IV) ions. ILs have been widely used as a sensitizer in CL studies. For example, Baader et al. had reported that peroxyoxalate CL could be enhanced in the presence of [BMIM][BF$_4$], as the quantum yield of the CL emitter was increased in the mixture solution of water and ILs.[40] The enhancement of Ce(IV)/CDP-star CL by ILs might follow a similar mechanism.

With the aid of [BMIM][BF$_4$], the sensitive detection of Ce(IV) ions was demonstrated. Figure 3 shows the CL intensities of 25 μM CDP-star and 2% (v/v) [BMIM][BF$_4$] with the addition of different concentrations of Ce(IV) ions. The CL intensity increased with increasing concentrations of Ce(IV) ions in the range from 0.5 to 100 μM, and a detection limit of 460 nM was obtained (Figure S7). The result shows
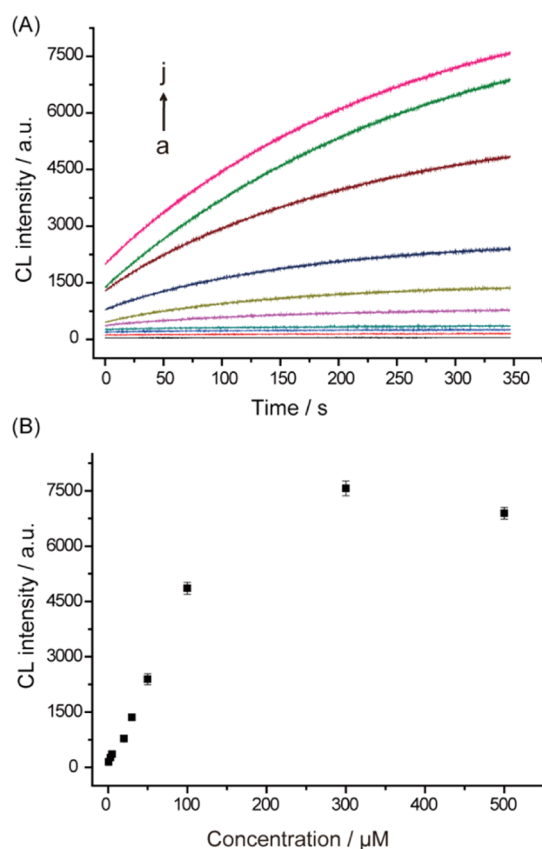
that the addition of [BMIM][BF$_4$] could greatly improve the sensitivity of the Ce(IV)/CDP-star CL system. Traditional methods for Ce(IV) ion detection include atomic emission spectrometry, fluorescence analysis, and electrochemical methods.[41,42] Compared with these methods, the presented CL method for Ce(IV) ion detection shows advantages such as easy operation and high sensitivity.

The selectivity of the CL method for Ce(IV) ion detection was also studied. Figure 4 shows the CL intensity of 25 μM CDP-star in the presence of different metal ions. The CL intensity of CDP-star was greatly increased after the addition of 100 μM Ce(IV) ions. In contrast, the addition of 1 mM other common metal ions showed a negligible effect on the CL of CDP-star. In Figure 4A, the CL signals of CDP-star in the presence of other metal ions were too weak to be observed. Therefore, the original data are given in the amplified version in Figure S8. All of these data suggest the excellent selectivity of the CL method for Ce(IV) ion detection. The high selectivity of the method is attributed to the intrinsic phosphatase-like activity of Ce(IV) ions, while other tested metal ions do not have the phosphatase-like activity.

CL Detection of AA and ClO$^-$. Due to the reversible redox switch between Ce(III) and Ce(IV), the CL method could be used for the detection of AA and ClO$^-$. As shown in Figure 5A, the CL intensity of Ce(IV)/CDP-star was significantly decreased upon the addition of 6 μM AA. AA can reduce Ce(IV) ions into Ce(III) ions, which results in the decrease of the CL intensity. The phenomenon was further applied for the CL detection of AA. The CL intensity versus AA concentration is linear in a concentration range from 0.5 to 6 μM (Figure S9), and a detection limit of 0.26 μM was obtained. It should be noted that other antioxidants may also result in the decrease of Ce(IV)/CDP-star CL due to their reducibility. The effect of ClO$^-$ on the CL of the Ce(III)/CDP-star system was also investigated. As shown in Figure 5B, the mixture of 25 μM CDP-star and 100 μM Ce(III) ions showed almost no CL emission. However, strong CL emission was observed after adding 100 μM ClO$^-$ into the system. The CL increase is ascribed to the oxidation of Ce(III) ions into Ce(IV) ions by the strong oxidizing reagent ClO$^-$. The finding was then used for the CL detection of ClO$^-$. The CL intensity increased linearly with the ClO$^-$ concentrations from 5 to 150 μM (Figure S10), and the detection limit for ClO$^-$ was 1.26 μM. It should be noted that the CL of CDP-star can be reversibly operated due to the reversible switch between Ce(III) and Ce(IV). As shown in Figure S11, the cycled switch-on and switch-off of CDP-star CL was carried out by the cyclic treatment of ClO$^-$ and AA.

CL Antioxidant Sensing in Fruit Juices. Fruit juice is one kind of good exogenous source of natural antioxidants. The TAC value of fruit juices is usually tested to assess their health beneficial effects. As the antioxidants in fruit juices (AA and other reducing substances) can result in the decrease of the CL intensity of the Ce(IV)/CDP-star system due to their reducibility, the CL method could be used for evaluating the TAC values in fruit juices. To demonstrate the possibility, the TAC values of three kinds of commercial fruit juices were measured and the results were expressed in AA concentration. As shown in Table S2, the TAC values of orange, peach, and pear juices were 30.25, 38.65, and 19.96 mM, respectively. To further demonstrate the effectiveness of the CL method, the TAC values were also measured using the standard addition method. As shown in Table S2, the CL recoveries range from

Figure 3. (A) CL kinetic curves of 25 μM CDP-star in the presence of different concentrations of Ce(IV) ions and 2% (v/v) [BMIM][BF$_4$] (from bottom to top: 0, 0.5, 3, 5, 20, 30, 50, 100, 300, and 500 μM). (B) Corresponding CL intensities of 25 μM CDP-star in the presence of different concentrations of Ce(IV) ions and 2% (v/v) [BMIM]-[BF$_4$].
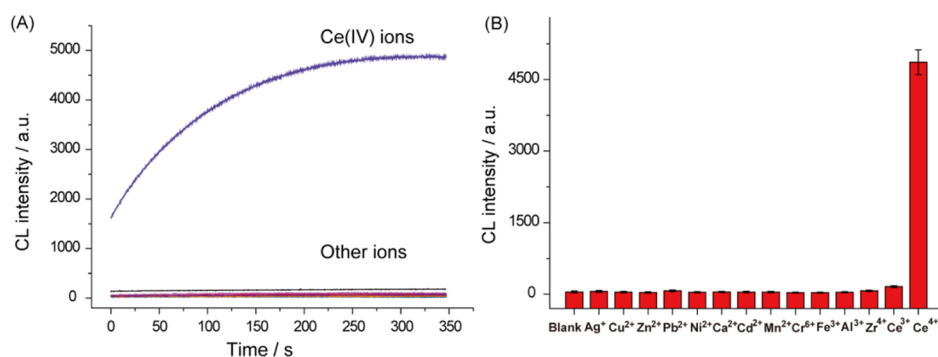
Figure 4. CL kinetic curves (A) and the corresponding histogram (B) of 25 μM CDP-star and 2% (v/v) [BMIM][BF$_4$] in the presence of different metal ions. The concentration of Ce(IV) ions was 100 μM while the concentrations of other metal ions were 1 mM.
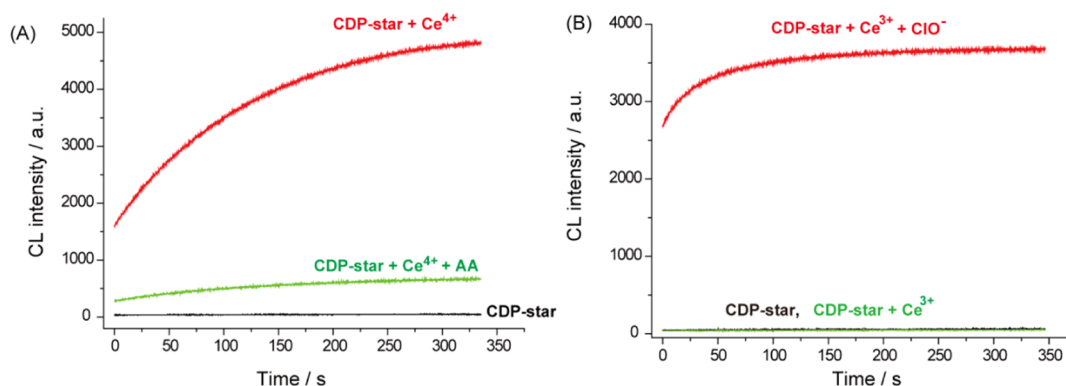
Figure 5. (A) CL kinetic curves of 25 μM CDP-star (black curve), 25 μM CDP-star with 100 μM Ce(IV) ions (red curve), and 25 μM CDP-star in the presence of 100 μM Ce(IV) ions and 6 μM AA (green curve). (B) CL kinetic curves of 25 μM CDP-star (black curve), 25 μM CDP-star with 100 μM Ce(III) ions (green curve), and 25 μM CDP-star in the presence 100 μM Ce(III) ions and 100 μM ClO$^-$ (red curve). The experiments were performed in 20 mM HEPES buffer (pH 7.0) containing 2% (v/v) [BMIM][BF$_4$].

95.58 to 102.57%. All of these data suggest that the CL method has great potential for the detection of TAC values in commercial fruit juices.

■ CONCLUSIONS

The Ce(IV)/CDP-star CL system was proposed based on the intrinsic phosphatase-like activity of Ce(IV) ions. The CL intensity of the Ce(IV)/CDP-star system can be significantly increased by the addition of ILs. The proposed Ce(IV)/CDP-star CL system was used for the detection of Ce(IV) ions with excellent selectivity. In addition, the CL detection of AA and ClO$^-$ was also demonstrated by utilizing the reversible Ce(III)/Ce(IV) switch. Due to the robust catalytic activity of Ce(IV) ions and the reversible Ce(III)/Ce(IV) switch, the Ce(IV)/CDP-star CL system shows great potential in the fields of Ce(IV) ion detection and redox-sensing.

■ EXPERIMENTAL SECTION

Materials and Instrumentation. CDP-star, alkaline phosphatase (ALP), 1-butyl-3-methylimidazolium tetrafluoroborate ([BMIM][BF$_4$]), and the malachite green phosphate assay kit were purchased from Sigma. Cerium(III) nitrate hexahydrate, ammonium cerium(IV) nitrate, and other metal salts were obtained from Sinopharm Chemical Reagent Co., Ltd. The solutions were prepared with water purified by a Milli-Q system.

CL data were collected from a CL analyzer (Xi'an Remex Analyse Instrument Co., Ltd). Absorption spectra were obtained on a UV-2550 UV—Vis spectrophotometer (Shi-

madzu, Japan). Fluorescence spectra were obtained on a PerkinElmer model LS-55 Luminescence spectrometer (PerkinElmer).

Procedure for the CL Assays. For the CL detection of Ce(IV) ions, different concentrations of Ce(IV) ions were added into 20 mM HEPES buffer (pH 7.0) containing 25 μM CDP-star and 2% (v/v) [BMIM][BF$_4$]. Then, the CL intensities of the mixtures were measured immediately at room temperature. The photomultiplier tube of the CL detector was set at a voltage of 600 V.

For the detection of AA, different amounts of AA were first mixed with 20 mM HEPES buffer (pH 7.0) containing 100 μM Ce(IV) ions and 2% (v/v) [BMIM][BF$_4$], and the mixtures were reacted for 10 min to ensure the reduction of Ce(IV) ions into Ce(III) ions. Then, 25 μM CDP-star was introduced into the solution, and the CL intensities of the solution were measured immediately. For the detection of ClO$^-$, different concentrations of ClO$^-$ were added into 20 mM HEPES buffer (pH 7.0) containing 100 μM Ce(III) ions and 2% (v/v) [BMIM][BF$_4$]. After 10 min, 25 μM CDP-star was added and the CL intensities were recorded. For commercial juice sample detection, the orange, peach, and pear juices were first diluted using 20 mM HEPES buffer (pH 7.0), then the diluted juice samples were measured following the procedure for AA sensing.

Kinetic Analysis and Relative Activity Comparison. The phosphatase-like activity of Ce(IV) ions was evaluated by steady-state kinetics. The reaction rates were obtained according to the speed of inorganic phosphate formation.

The concentration of inorganic phosphate was tested by a commercial malachite green phosphate assay kit. The experiments were carried out by mixing 100 μM Ce(IV) ions with different concentrations of CDP-star in 20 mM HEPES buffer (pH 7.0). After a reaction time of 2 minutes, the amounts of inorganic phosphate production were measured. The Michaelis−Menten constant and the maximal reaction velocity were calculated using the Lineweaver−Burk plot. The kinetic parameters of nanoceria particles and ALP were obtained by the same protocol.

■ ASSOCIATED CONTENT

ⓈⒾ Supporting Information

The Supporting Information is available free of charge at https://pubs.acs.org/doi/10.1021/acsomega.0c06301.

> Contains the effect of pH; kinetic parameters; linear plots; IL ratio; the reversibility studies; and the fruit juices' determination results (PDF)

■ AUTHOR INFORMATION

Corresponding Authors

Lianzhe Hu − *Chongqing Key Laboratory of Green Synthesis and Applications, College of Chemistry, Chongqing Normal University, Chongqing 401331, China;* ⓞ orcid.org/0000-0002-3639-1766; Email: lianzhehu@cqnu.edu.cn

Min Wang − *School of Pharmaceutical Sciences, Chongqing University, Chongqing 401331, China;* ⓞ orcid.org/0000-0002-5756-1015; Email: wang_min@cqu.edu.cn

Guobao Xu − *State Key Laboratory of Electroanalytical Chemistry, Changchun Institute of Applied Chemistry, Chinese Academy of Sciences, Changchun, Jilin 130022, China;* ⓞ orcid.org/0000-0001-9747-0575; Email: guobaoxu@ciac.ac.cn

Authors

Xilu Hu − *Chongqing Key Laboratory of Green Synthesis and Applications, College of Chemistry, Chongqing Normal University, Chongqing 401331, China*

Ting Huang − *School of Pharmaceutical Sciences, Chongqing University, Chongqing 401331, China*

Complete contact information is available at:
https://pubs.acs.org/10.1021/acsomega.0c06301

Notes

The authors declare no competing financial interest.

■ ACKNOWLEDGMENTS

■ ABBREVIATIONS USED

CDP-star:disodium 2-chloro-5-(4-methoxyspiro{1,2-dioxetane-3,2′-(5′-chloro)tricyclo[3.3.1.1^{3,7}]decan}-4-yl) phenyl phosphate

■ REFERENCES

(1) Han, Z.; Shu, J.; Jiang, Q.; Cui, H. Coreactant-free and label-Free eletrochemiluminescence immunosensor for copeptin based on luminescent immuno-gold nanoassemblies. *Anal. Chem.* **2018**, *90*, 6064−6070.

(2) Huang, Y.; Gao, L.; Cui, H. Assembly of multifunctionalized gold nanoparticles with chemiluminescent, catalytic, and immune activity for label-free immunoassays. *ACS Appl. Mater. Interfaces* **2018**, *10*, 17040−17046.

(3) Saqib, M.; Lou, B.; Halawa, M. I.; Kitte, S. A.; Liu, Z.; Xu, G. Chemiluminescence of lucigenin−allantoin and its application for the detection of allantoin. *Anal. Chem.* **2017**, *89*, 1863−1869.

(4) Kong, W.; Zhao, X.; Zhu, Q.; Gao, L.; Cui, H. Highly chemiluminescent magnetic beads for label-free sensing of 2,4,6-trinitrotoluene. *Anal. Chem.* **2017**, *89*, 7145−7151.

(5) Gao, W.; Wang, C.; Muzyka, K.; Kitte, S. A.; Li, J.; Zhang, W.; Xu, G. Artemisinin-luminol chemiluminescence for forensic blood-stain detection using a smart phone as a detector. *Anal. Chem.* **2017**, *89*, 6160−6165.

(6) Chen, G.; Jin, M.; Du, P.; Zhang, C.; Cui, X.; Zhang, Y.; Wang, J.; Jin, F.; She, Y.; Shao, H.; Wang, S.; Zheng, L. A review of enhancers for chemiluminescence enzyme immunoassay. *Food. Agr. Immunol.* **2017**, *28*, 315−327.

(7) Yang, Z.; Cao, Y.; Li, J.; Lu, M.; Jiang, Z.; Hu, X. Smart CuS nanoparticles as peroxidase mimetics for the design of novel label-free chemiluminescent immunoassay. *ACS Appl. Mater. Interfaces* **2016**, *8*, 12031−12038.

(8) Du, F.; Ma, X.; Yuan, F.; Wang, C.; Snizhko, D.; Guan, Y.; Xu, G. Sonochemiluminescence based on a small, cheap, and low-power USB mesh-type piezoelectric ultrasonic transducer. *Anal. Chem.* **2020**, *92*, 4755−4759.

(9) Lan, Y.; Yuan, F.; Fereja, T. H.; Wang, C.; Lou, B.; Li, J.; Xu, G. Chemiluminescence of lucigenin/riboflavin and its application for selective and sensitive dopamine detection. *Anal. Chem.* **2019**, *91*, 2135−2139.

(10) Huertas-Pérez, J. F.; Moreno-González, D.; Airado-Rodríguez, D.; Lara, F. J.; García-Campaña, A. M. Advances in the application of chemiluminescence detection in liquid chromatography. *TrAC, Trends Anal. Chem.* **2016**, *75*, 35−48.

(11) Gao, W.; Qi, W.; Lai, J.; Qi, L.; Majeed, S.; Xu, G. Thiourea dioxide as a unique eco-friendly coreactant for luminol chemiluminescence in the sensitive detection of luminol, thiourea dioxide and cobalt ions. *Chem. Commun.* **2015**, *51*, 1620−1623.

(12) Hananya, N.; Shabat, D. A glowing trajectory between bio- and chemiluminescence: from luciferin-based probes to triggerable dioxetanes. *Angew. Chem., Int. Ed.* **2017**, *56*, 16454−16463.

(13) Gu, B.; Dong, C.; Shen, R.; Qiang, J.; Wei, T.; Wang, F.; Lu, S.; Chen, X. Dioxetane-based chemiluminescent probe for fluoride ion-sensing in aqueous solution and living imaging. *Sens. Actuators, B* **2019**, *301*, No. 127111.

(14) Hananya, N.; Press, O.; Das, A.; Scomparin, A.; Satchi-Fainaro, R.; Sagi, I.; Shabat, D. Persistent chemiluminescent glow of phenoxy-dioxetane luminophore enables unique CRET-based detection of proteases. *Chem. - Eur. J.* **2019**, *25*, 14679−14687.

(15) Hananya, N.; Reid, J. P.; Green, O.; Sigman, M. S.; Shabat, D. Rapid chemiexcitation of phenoxy-dioxetane luminophores yields ultrasensitive chemiluminescence assays. *Chem. Sci.* **2019**, *10*, 1380−1385.

(16) Hananya, N.; Shabat, D. Recent advances and challenges in luminescent imaging: bright outlook for chemiluminescence of dioxetanes in water. *ACS Cent. Sci.* **2019**, *5*, 949−959.

(17) Gnaim, S.; Green, O.; Shabat, D. The emergence of aqueous chemiluminescence: new promising class of phenoxy 1,2-dioxetane luminophores. *Chem. Commun.* **2018**, *54*, 2073−2085.

(18) Wei, H.; Wang, E. Nanomaterials with enzyme-like characteristics (nanozymes): next-generation artificial enzymes. *Chem. Soc. Rev.* **2013**, *42*, 6060−6093.

(19) Wu, J.; Wang, X.; Wang, Q.; Lou, Z.; Li, S.; Zhu, Y.; Qin, L.; Wei, H. Nanomaterials with enzyme-like characteristics (nanozymes): next-generation artificial enzymes (II). *Chem. Soc. Rev.* **2019**, *48*, 1004−1076.

(20) Liu, B.; Liu, J. Surface modification of nanozymes. *Nano Res.* **2017**, *10*, 1125−1148.

(21) Wang, X.; Hu, Y.; Wei, H. Nanozymes in bionanotechnology: from sensing to therapeutics and beyond. *Inorg. Chem. Front.* **2016**, *3*, 41−60.

(22) Lin, Y.; Ren, J.; Qu, X. Catalytically active nanomaterials: A promising candidate for artificial enzymes. *Acc. Chem. Res.* **2014**, *47*, 1097−1105.

(23) Zhou, Y.; Liu, B.; Yang, R.; Liu, J. Filling in the gaps between nanozymes and enzymes: challenges and opportunities. *Bioconjugate Chem.* **2017**, *28*, 2903−2909.

(24) Hu, L.; Liao, H.; Feng, L.; Wang, M.; Fu, W. Accelerating the peroxidase-like activity of gold nanoclusters at neutral pH for colorimetric detection of heparin and heparinase activity. *Anal. Chem.* **2018**, *90*, 6247−6252.

(25) Gao, L.; Zhuang, J.; Nie, L.; Zhang, J.; Zhang, Y.; Gu, N.; Wang, T.; Feng, J.; Yang, D.; Perrett, S.; Yan, X. Intrinsic peroxidase-like activity of ferromagnetic nanoparticles. *Nat. Nanotechnol.* **2007**, *2*, 577−583.

(26) Liao, H.; Liu, G.; Liu, Y.; Li, R.; Fu, W.; Hu, L. Aggregation-induced accelerating peroxidase-like activity of gold nanoclusters and their applications for colorimetric Pb^{2+} detection. *Chem. Commun.* **2017**, *53*, 10160−10163.

(27) Deng, H.-H.; Lin, X.-L.; Liu, Y.-H.; Li, K.-L.; Zhuang, Q.-Q.; Peng, H.-P.; Liu, A.-L.; Xia, X.-H.; Chen, W. Chitosan-stabilized platinum nanoparticles as effective oxidase mimics for colorimetric detection of acid phosphatase. *Nanoscale* **2017**, *9*, 10292−10300.

(28) Duan, D.; Fan, K.; Zhang, D.; Tan, S.; Liang, M.; Liu, Y.; Zhang, J.; Zhang, P.; Liu, W.; Qiu, X.; Kobinger, G. P.; Gao, G. F.; Yan, X. Nanozyme-strip for rapid local diagnosis of Ebola. *Biosens. Bioelectron.* **2015**, *74*, 134−141.

(29) Kuchma, M. H.; Komanski, C. B.; Colon, J.; Teblum, A.; Masunov, A. E.; Alvarado, B.; Babu, S.; Seal, S.; Summy, J.; Baker, C. H. Phosphate ester hydrolysis of biologically relevant molecules by cerium oxide nanoparticles. *Nanomedicine* **2010**, *6*, 738−744.

(30) Yao, T.; Zhimin, T.; Zhang, Y.; Qu, Y. Phosphatase-like activity of porous nanorods of CeO_2 for the highly stabilized dephosphorylation under interferences. *ACS Appl. Mater. Interfaces* **2019**, *11*, 195−201.

(31) Xu, F.; Lu, Q.; Huang, P.-J. J.; Liu, J. Nanoceria as a DNase I mimicking nanozyme. *Chem. Commun.* **2019**, *55*, 13215−13218.

(32) Liu, H.; Liu, J. Self-limited phosphatase-mimicking CeO_2 nanozymes. *ChemNanoMat* **2020**, *6*, 947−952.

(33) Manto, M. J.; Xie, P.; Wang, C. Catalytic dephosphorylation using ceria nanocrystals. *ACS Catal.* **2017**, *7*, 1931−1938.

(34) Tian, X.; Liao, H.; Wang, M.; Feng, L.; Fu, W.; Hu, L. Highly sensitive chemiluminescent sensing of intracellular Al^{3+} based on the phosphatase mimetic activity of cerium oxide nanoparticles. *Biosens. Bioelectron.* **2020**, *152*, No. 112027.

(35) Hu, L.; Deng, L.; Alsaiari, S.; Zhang, D.; Khashab, N. M. "Light-on" sensing of antioxidants using gold nanoclusters. *Anal. Chem.* **2014**, *86*, 4989−4994.

(36) Wang, J.; Ni, Y.; Shao, S. A reversible fluorescence probe for detection of $ClO^−$/AA redox cycle in aqueous solution and in living cells. *Talanta* **2016**, *147*, 468−472.

(37) Rauf, S.; Ali, N.; Tayyab, Z.; Shah, M. Y.; Yang, C. P.; Hu, J.; Kong, W.; Huang, Q.; Hayat, A.; Muhammad, N. Ionic liquid coated zerovalent manganese nanoparticles with stabilized and enhanced peroxidase-like catalytic activity for colorimetric detection of hydrogen peroxide. *Mater. Res. Express* **2020**, *7*, No. 035018.

(38) Lin, Y.; Zhao, A.; Tao, Y.; Ren, J.; Qu, X. Ionic liquid as an efficient modulator on artificial enzyme system: toward the realization of high-temperature catalytic reactions. *J. Am. Chem. Soc.* **2013**, *135*, 4207−4210.

(39) Rauf, S.; Nawaz, M. A. H.; Muhammad, N.; Raza, R.; Shahid, S. A.; Marty, J. L.; Hayat, A. Protic ionic liquids as a versatile modulator and stabilizer in regulating artificial peroxidase activity of carbon materials for glucose colorimetric sensing. *J. Mol. Liq.* **2017**, *243*, 333−340.

(40) Cabello, M. C.; El Seoud, O. A. A.; Baader, W. J. Effect of ionic liquids on the kinetics and quantum efficiency of peroxyoxalate chemiluminescence in aqueous media. *J. Photochem. Photobiol., A* **2018**, *367*, 471−478.

(41) Huang, L.; Liu, Y.; Ma, C.; Xi, P.; Kou, W.; Zeng, Z. A fluorescent probe for the determination of Ce^{4+} in aqueous media. *Dyes Pigm.* **2013**, *96*, 770−773.

(42) Lai, X.; Wang, R.; Li, J.; Qiu, G.; Liu, J. A cascade reaction-based switch-on fluorescent sensor for Ce(IV) ions in real samples. *RSC Adv.* **2019**, *9*, 22053−22056.